Journal of Visualized Experiments

A Neuronal Apoptosis Model induced by Spinal Cord Compression in Rat

--Manuscript Draft--

Article Type:	Methods Article - JoVE Produced Video
Manuscript Number:	JoVE62604R2
Full Title:	A Neuronal Apoptosis Model induced by Spinal Cord Compression in Rat
Corresponding Author:	Xue-Jun Cui, Ph.D Longhua Hospital,Shanghai university of Traditional Chinese Medicine Shang Hai, China CHINA
Corresponding Author's Institution:	Longhua Hospital,Shanghai university of Traditional Chinese Medicine
Corresponding Author E-Mail:	13917715524@139.com
Order of Authors:	Xue-Jun Cui, Ph.D
	Yue-li Sun
	Gan Li
	Zhong Zheng
	Min Yao
	Shu-fen Liu
	Jia-wen Cui
	Kim Sia Sng
	Long-yun Zhou
	Yong-jun Wang
Additional Information:	
Question	**Response**
Please specify the section of the submitted manuscript.	Biology
Please indicate whether this article will be Standard Access or Open Access.	Open Access ($3900)
Please indicate the **city, state/province, and country** where this article will be **filmed**. Please do not use abbreviations.	ShangHai，China
Please confirm that you have read and agree to the terms and conditions of the author license agreement that applies below:	I agree to the Author License Agreement
Please provide any comments to the journal here.	

TITLE:

A Neuronal Apoptosis Model induced by Spinal Cord Compression in Rat

AUTHORS AND AFFILIATIONS:

Yue-li Sun[1,2,#], Gan Li[1,2,#], Zhong Zheng[1,2,#], Min Yao[1,2], Jia-Wen Cui[1,2,3], Shu-fen Liu[1,2], Long-Yun Zhou[1,2], Kim-Sia Sng[1,2], Xue-jun Cui[1,2], Yong-jun Wang[1,2,3]

[1]Longhua Hospital, Shanghai University of Traditional Chinese Medicine, Shanghai 200032, China
[2]Spine Research Institute, Shanghai University of Traditional Chinese Medicine, Shanghai 200032, China
[3]Shanghai University of Traditional Chinese Medicine, Shanghai 201203, China

# YL Sun, G Li, and Z Zheng contributed equally to this paper

Email addresses of co-authors:

Yue-li Sun	yueli_sun@foxmail.com
Gan Li	493224468@qq.com
Zhong Zheng.	757578713@qq.com
Min Yao	yaomin19871223@126.com
Jia-Wen Cui	cuijiawen2011@163.com
Shu-Fen Liu.	xiaoliufenfen@139.com
Long-Yun Zhou	228970442@qq.com
Kim-Sia Sng	kimsiasng@hotmail.com
Xue-jun Cui	13917715524@139.com
Yong-jun Wang	yjwang8888@126.com

Corresponding authors:

Xue-jun Cui.	13917715524@139.com
Yong-jun Wang	yjwang8888@126.com

KEYWORDS:

cervical spondylotic myelopathy, spinal cord compression, neuronal apoptosis, rat, animal model, protocol

SUMMARY:

Here, we present a protocol to generate a rat spinal cord compression model, assess its behavioral score, and observe the compressed spinal cord region. The behavioral assessments showed decreased monitor motor disability. Hematoxylin and eosin staining and immunostaining revealed considerable neuronal apoptosis in the compressed region of the spinal cord.

ABSTRACT:

As a severe progressive degenerative disease, cervical spondylotic myelopathy (CSM) has a poor prognosis and is associated with physical pain, stiffness, motor or sensory dysfunction, and a high risk of spinal cord injury and acroparalysis. Thus, therapeutic strategies that

promote efficient spinal cord regeneration in this chronic and progressive disease are urgently needed. Effective and reproducible animal spinal cord compression models are required to understand the complex biological mechanism underlying CSM. Most spinal cord injury models reflect acute and structural destructive conditions, whereas animal models of CSM present a chronic compression in the spinal cord. This paper presents a protocol to generate a rat spinal cord compression model, which was further evaluated by assessing the behavioral score and observing the compressed spinal cord region. The behavioral assessments showed decreased monitor motor disability, including joint movements, stepping ability, coordination, trunk stability, and limb muscle strength. Hematoxylin and eosin (H&E) staining and immunostaining revealed considerable neuronal apoptosis in the compressed region of the spinal cord.

INTRODUCTION:

As a common progressive degenerative disease, CSM accounts for 5–10% of all cervical spondylosis[1]. If patients suffering from CSM ignore their symptoms and fail to treat them in a timely and effective manner, this could lead to severe complications, such as spinal cord injury and limb paralysis, which would deteriorate with aging, posing a substantial economic and mental burden to patients and their families[2,3]. The pathogenesis of CSM is complex, involving static and dynamic factors, the hypoxia-ischemia theory, endothelial cell injury, the blood spinal cord barrier destruction theory, and the inflammation and apoptosis theory[4,5,6,7].

The static and dynamic mechanisms of compression on the spinal cord cause clinical symptoms. Protruding vertebral discs, deformed vertebral bodies, and calcified ligaments may cause prolonged spinal cord compression, which will gradually affect the blood-spinal cord barrier and local microvasculature in the spinal cord[4,8]. In turn, ischemia, inflammation, and apoptosis affect the neurons, axons, and glial cells[6,9].

The experimental animal models of spinal cord injury include contusive injury, compressive injury, traction injury, photochemical-induced injury, and ischemia-reperfusion injury. Most of these models also reflect some acute and structural destructive conditions (transection or chemical toxicity). However, these animal models of CSM cannot present progressive neuronal apoptosis in the spinal cord.

This paper describes a detailed protocol to generate a rat spinal cord compression model, which was further evaluated by assessing the behavioral score and observing the compressed region of the spinal cord. This rat spinal cord compression model is a reliable animal model for further investigation of the mechanisms involved in CSM.

PROTOCOL:

The following procedure was performed with approval from the Institutional Animal Care and Use Committee (IACUC), Shanghai University of Traditional Chinese. All survival surgeries were performed under sterile conditions as outlined by the NIH guidelines. Pain and risk of infections were managed with appropriate analgesics and antibiotics to ensure a successful outcome. This surgical procedure is optimized for Sprague–Dawley (SD) outbred male rats at 12 weeks of age and 400 g weight.

1. PVA-polyacrylamide hydrogel preparation

NOTE: As shown in **Figure 1G,H**, the PVA-polyacrylamide hydrogel is a water-absorbing polymer sheet. In the natural state, the gel is extremely difficult to cut into small pieces. The preparation is described as follows.

1.1. Place a PVA-polyacrylamide hydrogel in water for 24 h to make it easier to cut after hydration.

1.2. Use a self-made cutting tool (**Figure 1H**) to divide the whole hydrogel into pieces, sized 2 mm x 2 mm x 2 mm.

1.3. Transfer these hydrogel pieces to an oven at 60 °C for 12 h for dehydration into small pieces of 1 mm x 1 mm x 1 mm as implantation materials.

2. Anesthesia and preparation

NOTE: Be sure to wear a surgical cap, disposable medical masks, and sterile surgical gloves throughout the sterile surgical process.

2.1. Place the rat on a heating pad, and ensure that rectal temperature is maintained at 37±1 °C during anesthesia.

2.2. Place the rat into the anesthesia chamber filled with 3% isoflurane for ~3 min.

2.3. Gently pinch the rat's limbs and toes with tweezers to test for loss of withdrawal response, indicating successful anesthetization.

2.4. Fix the rat on the operating table in a prone position, ensuring that the limbs and head of the rat are firmly fixed.

2.5. Fix the anesthesia mask to the face of the rat. Administer 2% isoflurane in an oxygen/air mixture via a standard rat nose mask to anesthetize the rat throughout the spinal compression surgery.

2.6. Place a cylindrical gauze pad (size of about 30 mm x 20 mm x 60 mm) between the rat and the operating table (**Figure 1A**) to ensure an unobstructed airway and fully exposed surgical site throughout the surgery.

2.7. Shave the hair around the surgical area of the rat's neck with an electric shaver.

2.8. Apply depilating cream to remove the remaining hair and expose the skin.

2.9. Disinfect the surgical area with iodophor.

2.10. Cover the disinfected area with a sterile towel with a hole exposing only the surgical area on the dorsal side of the rat's neck.

3. Surgical approach

3.1. Percutaneously positioning the second cervical spinous process and second thoracic spinous process, make a longitudinal incision in the dorsal midline with a scalpel from the second cervical spinous process to the second thoracic spinous process.

3.2. Move the obtuse muscles of both sides with hemostatic forceps to expose the C2-T2 lamina after cutting subcutaneous tissue and fascia layer by layer.

3.3. Remove the ligamentum flavum between the C2-T2 lamina of the right side using microscopic shears, and separate the lamina to expose the dura mater (**Figure 1B**).

3.4. Separate the dural membranes carefully from the lamina using toothed forceps to expose the space beneath the lamina.

3.5. Drill a hole (1 mm x 1 mm) on the cervical laminar.

NOTE: To avoid excessive injury on the spinal cord, ensure that the rat's neck is maintained in a dorsal arch state, allowing sufficient space between the cervical laminas.

3.6. Use microsurgical forceps to grasp a piece of PVA-polyacrylamide hydrogel of the size of 1 mm x 1 mm x 1 mm and insert it into the previously drilled hole (**Figure 1C,D**).

NOTE: Transient twitching performance indicates the spinal cord compression model has been established successfully.

3.7. Suture the muscle, fascia, subcutaneous, and skin tissues, layer by layer, using triangular needles and 5-0 suture.

3.8. After disinfection, transfer the animals back to the cage and keep them warm.

3.9. Subcutaneously inject buprenorphine hydrochloride analgesia (0.03 mg/kg) every 6 h for 3 days following the surgery and as needed after that.

4. Postoperative management

4.1. Inject an equivalent of 100,000 units of penicillin intraperitoneally into the rats once a day to prevent postoperative infection and relieve pain.

4.2. Transfer the rats to new cages that have been continuously heated with an infrared lamp to ensure adequate heat preservation postoperatively.

NOTE: Remove the heating lamp after the rat's consciousness is restored

4.3. Maintain hygiene and ventilation of the rat's feeding cage.

4.4. Assist the rats with eating and drinking twice a day. If necessary, administer a bladder massage to assist in urination until the urinary function is restored.

5. Behavioral assessment

5.1. Use the Basso, Beattie, and Bresnahan (BBB) rating scale to assess postoperative behavior.

NOTE: The BBB rating scale is a gold standard (**Table 1**) used to evaluate spinal cord-related function in rats. It assesses rats' movement according to scores ranging from 0 (no hind limb movement was observed) to 21 (gait coordination, toe space consistency, main claw position parallel in the whole posture, consistent trunk stability, and consistent tail elevation).

6. Grip strength test

6.1. Use an electronic grip strength meter to measure grip strength.

6.1.1. Grab the lower half of the rat to suspend the rat and allow it to grab the metal rod of the front grip meter.

6.1.2. When the rat grasps the metal rod, pull it away and record the grip strength.

6.1.3. Measure the grip strength three times for each rat and record the highest score.

7. Inclined plate test

7.1. Place the rat on a rubber plate with an adjustable angle.

7.2. Gradually raise the inclined plate angle by 5° each time until the rat manages to balance and stand firm for 5 s.

7.3. Record the maximum angle at which the rat can balance itself on the inclined plate.

7.4. Measure the maximum angle three times for each rat and record the highest score.

8. Euthanasia, spinal cord separation, and frozen embedding

NOTE: Ensure that appropriate eye goggles and face shield/mask are worn to protect the eyes, face, and respiratory tract from paraformaldehyde and formaldehyde gas.

8.1. Inject an equivalent of 10% chloral hydrate intraperitoneally to anesthetize the rats before opening the sternum to expose the heart.

8.2. Insert a perfusion needle into the apex of the heart, fix it with hemostatic forceps, and slowly infuse with normal saline.

8.3. Drill a hole on the right atrial appendage until clean normal saline flows out of the right atrium, indicating a successful infusion.

8.4. Inject normal saline to expand the volume of the heart.

8.5. Cut the right auricular appendage with scissors to let the blood flow out with normal saline, indicating complete systemic circulation.

8.6. Stop the normal saline perfusion after the liver turns white.

8.7. Infuse with an equivalent of 10% paraformaldehyde until the rat's body becomes stiff.

8.8. After paraformaldehyde perfusion, remove the skin, muscles, and soft tissues around the spine; separate the C2–C7 segment of the cervical spine; and immerse it into 10% paraformaldehyde for fixation overnight.

8.9. Separate the cervical spinal cord from the spine and place it into a concentration gradient of 10%, 20%, and 30% sucrose solutions for gradual dehydration.

8.10. Transfer the compressed spinal cord of 2 mm height along with an OCT embedding agent into a -80 °C freezer.

8.11. After sectioning into 7-µm-thick slices and staining (H&E staining and dUTP nick end labeling (TUNEL)/neuronal nuclei (NeuN), see section 9), observe the histopathology of the spinal cord and neuronal apoptosis, respectively.

9. TUNEL/NeuN immunostaining

9.1. Immerse the spinal cord sections in 1.2% hydrogen peroxide for 20 min at room temperature to inhibit the endogenous peroxidase activity.

9.2. Incubate the spinal cord sections with a rabbit polyclonal anti-NeuN antibody (diluted 1:500;) and perform the one-step TUNEL apoptosis assay (green fluorescence) in phosphate-buffered saline with 0.3% Triton X-100 overnight at 4 °C.

9.3. Incubate the spinal cord sections with biotinylated anti-rabbit IgG secondary antibody for 2 h at room temperature.

9.4. Immerse the spinal cord sections with 3,3'-diaminobenzidine solution (0.06% DAB agar) in 0.01 M PBS buffer (100 mL) and 30% hydrogen peroxide (50 µL) for 1 min to visualize the immune reactions.

REPRESENTATIVE RESULTS:

Spinal cord compressive injury may lead to neuromuscular disability in limbs

As the hydrogel piece expands gradually, it persistently compresses the spinal cord region for a prolonged period, which simulates the forelimb disabilities induced by cervical spinal cord diseases[8,10]. In the current model, considerable ipsilateral forepaw contracture was observed

in most of the rats (9/10) in the model group (**Figure 2A**). Further measurement and analysis of the forepaws' length and width were conducted on a piece of paper with a grid line (**Figure 2B**). The data revealed that the length and width of the ipsilateral forepaws in the model group were remarkably decreased one day post-surgery ($P < 0.01$). However, no significant difference was detected in the contralateral forepaws between the control and model groups (**Figure 2C**).

To evaluate the progress and neuromuscular disability in limbs, the BBB rating scale, inclined plane test, and forelimb grip test were employed for observation on days 1, 3, 7, 14, 21, and 28 after the surgery. One-way or two-way analysis with Tukey's test was performed to analyze normally distributed data. A nonparametric Mann-Whitney *U*-test with *post hoc* analysis was performed for data that were not normally distributed but contained equal variances. Data are expressed as mean ± standard deviation (SD). Differences were considered statistically significant at $P < 0.05$.

The results showed that the BBB scores of the rats in the model group gradually decreased on days 1 and 3 after the surgery, presenting significant functional disability during the early phase, especially on the ipsilateral side (**Figure 2D,E** and **Figure 2G**). Although recovery for spinal cord compression was observed in both the model and control groups, the rats in the model group showed a tardy and incomplete recovery of the aberrant forepaw function and balancing ability compared to the control group at 4 weeks post-surgery (**Figure 2E** and **Figure 2G**). Significant differences between the model and control groups were maintained in the inclined plane score and grip strength on day 28 post-surgery. These combined results indicate that this surgery induces progressive compression on the cervical spinal cord and causes deterioration of motor ability in rats.

Histological changes and inflammation induced by compression in the spinal cord

After separating the cervical spinal cord, a prominent indentation of 2 mm depth and 2 mm x 2 mm area could be observed on the spinal cord (**Figure 3B**). To assess the morphometric changes, the spinal cord sections were stained and viewed under a light microscope. The H&E staining revealed the infiltration of immune cells and a dramatic loss of neurons in the compressive region of the spinal cord (**Figure 3C**). In addition, the immunostaining revealed a dramatic increase in neuronal apoptosis in the spinal cord compression site in the model group (**Figure 3D,E**). Some cells or tissues have high nuclease and polymerase activity levels, which could result in nonspecific fluorescence. Hence, the tissue was immobilized immediately after it was extracted to prevent these enzymes from causing false positives. TUNEL staining is nonspecific and can be employed in the event of cell or neuron death. NeuN is a specific staining marker for neurons. As a result, merged images from TUNEL staining and NeuN staining were used to demonstrate neuronal apoptosis.

FIGURE AND TABLE LEGENDS:

Figure 1: A schematic of the surgical procedure. (**A**) A gauze pad was placed under the rat to ensure that the airway of the rat was clear during the operation. (**B–D**) A surgical procedure of hydrogel implantation into the cervical spinal canal; the yellow arrowhead points to a tiny hole drilled on the vertebral plate of C6, and the green arrowhead indicates the dehydrated hydrogel block**.** (**E**) A schematic of the surgical procedure. (**F**) A three-dimensional schematic

of spinal cord compression. (**G**) Water-absorbing property of the PVA-polyacrylamide hydrogel. (**H**) Preparation of the hydrogel block for spinal cord compression. Abbreviations: PVA = polyvinyl alcohol.

Figure 2: Morphology of the forepaw and behavioral observations with BBB scale, grip strength test, and inclined plate test. (**A**) A typical feature of the ipsilateral forepaws of the control group (left) and model group (right) rats on the third day after surgery. (**B**) The width and length of the forepaws of the rats were measured. The transverse red arrow is from the first finger to the fourth finger, and the longitudinal red arrow is from the tip of the longest finger to the root of the palm. (**C**) Quantitative analysis of the length and width of the ipsilateral forepaws in the model and control groups. (**D**) BBB score of both the ipsilateral and contralateral sides 1, 3, 7, 14, 21, and 28 days after surgery. (**E**) The grip strength of both the ipsilateral and contralateral side forelimbs 1, 3, 7, 14, 21, and 28 days after surgery, assessed with the grip strength test. (**F**) Schematic of the inclined plate test. (**G**) The strength and balance of both ipsilateral side and contralateral side limbs 1, 3, 10, 20, and 28 days after surgery, assessed with the inclined plate test. Data are presented as mean ± SD. *P < 0.05 and **P < 0.01 vs. control group; n = 10/group. Abbreviation: BBB = Basso, Beattie, and Bresnahan rating scale.

Figure 3: Morphological changes and inflammatory responses after prolonged cervical spinal cord compression. (**A**) A three-dimensional schematic of spinal cord compression. (**B**) An indentation of 2 mm depth and 2 mm x 2 mm-area on the spinal cord. (**C**) A spinal cord histological section at 28 days after compression and H&E staining. The infiltration of immune cells and a dramatic loss of neurons in the compressive region of the spinal cord. Red rectangle, ipsilateral side; green rectangle, contralateral; blue arrowheads, immune cells; yellow arrows, neurons. (**D**) Double staining for NeuN (red)/TUNEL (green) of sections from the spinal cord compression site in the model and control groups. Scale bars = 20 μm. (**E**) Quantification of NeuN and TUNEL double-positive cells. ***P < 0.001 compared to the control group; n = 10/group. Abbreviations: H & E = hematoxylin and eosin; NeuN = neuronal nuclei; TUNEL = dUTP nick end labeling.

Table 1: 21-point functional evaluation scale of Basso et al.[9,11].

DISCUSSION:

The goal of this surgical procedure was to generate reproducible, prolonged, inflammatory infiltration in the rat spinal cord. A key advantage of this model is that the expandable hydrogel implants provide an initial blunt injury and subsequent inflammation in the spinal cord, thereby leading to a progressive inflammatory response (**Figure 2C**), which is consistent with the pathological process of CSM. In the current study, the mortality from spinal cord injury was extremely low (~2 in 50), whereas the repeatability of this model was > 45 in 50. Incorrect size of the hydrogel pieces and vigorous implantation during the surgery might cause an acute injury to the spinal cord[12,13].

An unpublished study[14] found that implantation with an expansion rate of 350% resulted in temporary and acute CSM with progressive recovery for several weeks. An expansion rate of 200% caused a slow progressive paralysis in the CSM model because the implants were harder than the spinal cord. However, in this model, we were not interested in the hardness of the

implanted material, only in the final size of this implantation. After 4 weeks, an indentation on the spinal cord (**Figure 3A,B**) was observed, which reflected the sustained constriction on the spinal cord, aggravated neuroinflammation, and neuronal apoptosis.

Currently, there is no consensus on the size of the implants. Several studies used absorbent sheets with a thickness of 0.5–1 mm[15,16,17,18] and reported functional disability from spinal compression. Another rat spinal cord compression study[19] showed that the loss of intact white matter and dramatic cord flattening were induced by severe cord compression (2.6 mm thickness), which reflected a compression strain without inflammation. Therefore, a large implant fabricated with a soft expandable material may be suitable for prolonged compression on the spinal cord.

In the current model, the size of the hydrogel pieces and drill on the vertebral plate was strictly limited to a size of 1 mm x 1 mm x 1 mm to avoid acute spinal cord injury or accidental death due to any sudden force due to oversized implants. After 48 h of hydration, the hydrogel blocks expanded to a size of 2 mm x 2 mm x 2 mm. Clinically, the aggravation of symptoms in CSM patients is related to the sudden compression of the spinal cord, which is from continuous disc herniated compression on the spinal cord and subsequent lower compensated adaptation induced by inflammation and edema[4,7]. This could explain why unilateral hydrogel inflammatory infiltration leads to a bilateral neurological function deficit[20].

One limitation of this animal model is that rats show strong adaptation to any injury[21], which facilitates quick recovery. Several studies have shown continuous improvements in neurological function over time after the compression operation[15,16,17,18,21,22,15-18,21,22], whereas only a few studies have reported a deteriorating trend. In addition, most CSM patients show either a gradual recovery or deterioration in neurological function under consistent compression on the spinal cord[23]. As there was no significant difference in the motor function in the current model after 4 weeks, we stopped the behavioral assessment and euthanized the rats for further histological investigations. In summary, this study presents a neural apoptosis model induced by spinal cord compression in rat, a practical animal model to study the cellular and molecular mechanisms associated with CSM and spinal cord regeneration.

ACKNOWLEDGMENTS:

This study was supported by the National Key R&D Program of China (2018YFC1704300), National Natural Science Foundation of China (81930116, 81804115, 81873317, and 81704096), Shanghai Sailing Program (18YF1423800). This project was also supported by the Shanghai University of Traditional Chinese Medicine (2019LK057).

DISCLOSURES:

The authors have no conflicts of interest to disclose and state that there are no restrictions on full access to all the materials used in this study.

REFERENCES:

1. Lebl, D. R., Bono, C. M. Update on the diagnosis and management of cervical spondylotic myelopathy. *The Journal of the American Academy of Orthopaedic Surgeons*. **23** (11), 648–660 (2015).

2. Haddas, R. et al. Spine and lower extremity kinematics during gait in patients with cervical spondylotic myelopathy. *The Spine Journal*. **18** (9), 1645–1652 (2018).
3. Song, D. W., Wu, Y. D. Tian, D. D. Association of Vdr-Foki and Vdbp-Thr420 Lys polymorphisms with cervical spondylotic myelopathy: A case-control study in the population of China. *Journal of Clinical Laboratory Analysis*. **33** (2), e22669 (2019).
4. Kurokawa, R., Murata, H., Ogino, M., Ueki, K., Kim, P. Altered blood flow distribution in the rat spinal cord under chronic compression. *Spine*. **36** (13), 1006–1009 (2011).
5. Wen, C. Y. et al. Is Diffusion anisotropy a biomarker for disease severity and surgical prognosis of cervical spondylotic myelopathy? *Radiology*. **270** (1), 197–204 (2014).
6. Long, H. Q., Li, G. S., Hu, Y., Wen, C. Y. Xie, W. H. Hif-1A/Vegf signaling pathway may play a dual role in secondary pathogenesis of cervical myelopathy. *Medical Hypotheses*. **79** (1), 82–84 (2012).
7. Karadimas, S. K., Erwin, W. M., Ely, C. G., Dettori, J. R., Fehlings, M. G. Pathophysiology and natural history of cervical spondylotic myelopathy. *Spine*. **38**, S21–S36 (2013).
8. Wilson, J. R. et al. State of the art in degenerative cervical myelopathy: an update on current clinical evidence. *Neurosurgery*. **80**, S33–S45 (2017).
9. Baptiste, D. C., Fehlings, M. G. Pathophysiology of cervical myelopathy. *The spine Journal*. **6**, 190S–197S (2006).
10. Wilcox, J. T. et al. Generating level-dependent models of cervical and thoracic spinal cord injury: exploring the interplay of neuroanatomy, physiology, and function. *Neurobiology of Disease*. **105**, 194–212 (2017).
11. Takano, M. et al. Inflammatory cascades mediate synapse elimination in spinal cord compression. *Journal of Neuroinflammation*. **11**, 40 (2014).
12. Hu, Y. et al. Somatosensory-evoked potentials as an indicator for the extent of ultrastructural damage of the spinal cord after chronic compressive injuries in a rat model. *Clinical Neurophysiology*. **122** (7), 1440–1447 (2011).
13. Yang, T. et al. Inflammation level after decompression surgery for a rat model of chronic severe spinal cord compression and effects on ischemia-reperfusion injury. *Neurologia Medico-Chirurgica*. **55** (7), 578–586 (2015).
14. Ijima, Y. et al. Experimental rat model for cervical compressive myelopathy. *Neuroreport*. **28** (18), 1239–1245 (2017).
15. Yamamoto, S., Kurokawa, R., Kim, P. Cilostazol, a selective type iii phosphodiesterase inhibitor: prevention of cervical myelopathy in a rat chronic compression model. *Journal of Neurosurgery. Spine*. **20** (1), 93–101 (2014).
16. Holly, L. T.et al. Dietary therapy to promote neuroprotection in chronic spinal cord injury. *Journal of Neurosurgery. Spine*. **17** (2), 134–140 (2012).
17. Zhao, P .et al. In vivo diffusion tensor imaging of chronic spinal cord compression: a rat model with special attention to the conus medullaris. *Acta Radiologica*. **57** (12), 1531–1539 (2016).
18. Kurokawa, R., Nagayama, E .,Murata, H., Kim, P. Limaprost alfadex, a prostaglandin E1 derivative, prevents deterioration of forced exercise capability in rats with chronic compression of the spinal cord. *Spine*. **36** (11), 865–869 (2011).
19. Lee J., Satkunendrarajah, K., Fehlings, M. G. Development and characterization of a novel rat model of cervical spondylotic myelopathy: the impact of chronic cord compression on clinical, neuroanatomical, and neurophysiological outcomes. *Journal of Neurotrauma*. **29** (5), 1012–1027 (2012).
20. Chen, B. et al. Reactivation of dormant relay pathways in injured spinal cord by Kcc2

manipulations. *Cell*. **174** (3), 521–535 (2018).
21. Yu, W. R., Liu, T., Kiehl, T. R., Fehlings, M. G. Human neuropathological and animal model evidence supporting a role for Fas-mediated apoptosis and inflammation in cervical spondylotic myelopathy. *Brain*. **134**, 1277–1292 (2011).
22. Yu, W. R. et al. Molecular mechanisms of spinal cord dysfunction and cell death in the spinal hyperostotic mouse: implications for the pathophysiology of human cervical spondylotic myelopathy. *Neurobiology of Disease*. **33** (2), 149–163 (2009).
23. Iyer, A., Azad, T. D. Tharin, S. Cervical spondylotic myelopathy. *Clinical Spine Surgery*. **29** (10), 408–414 (2016).

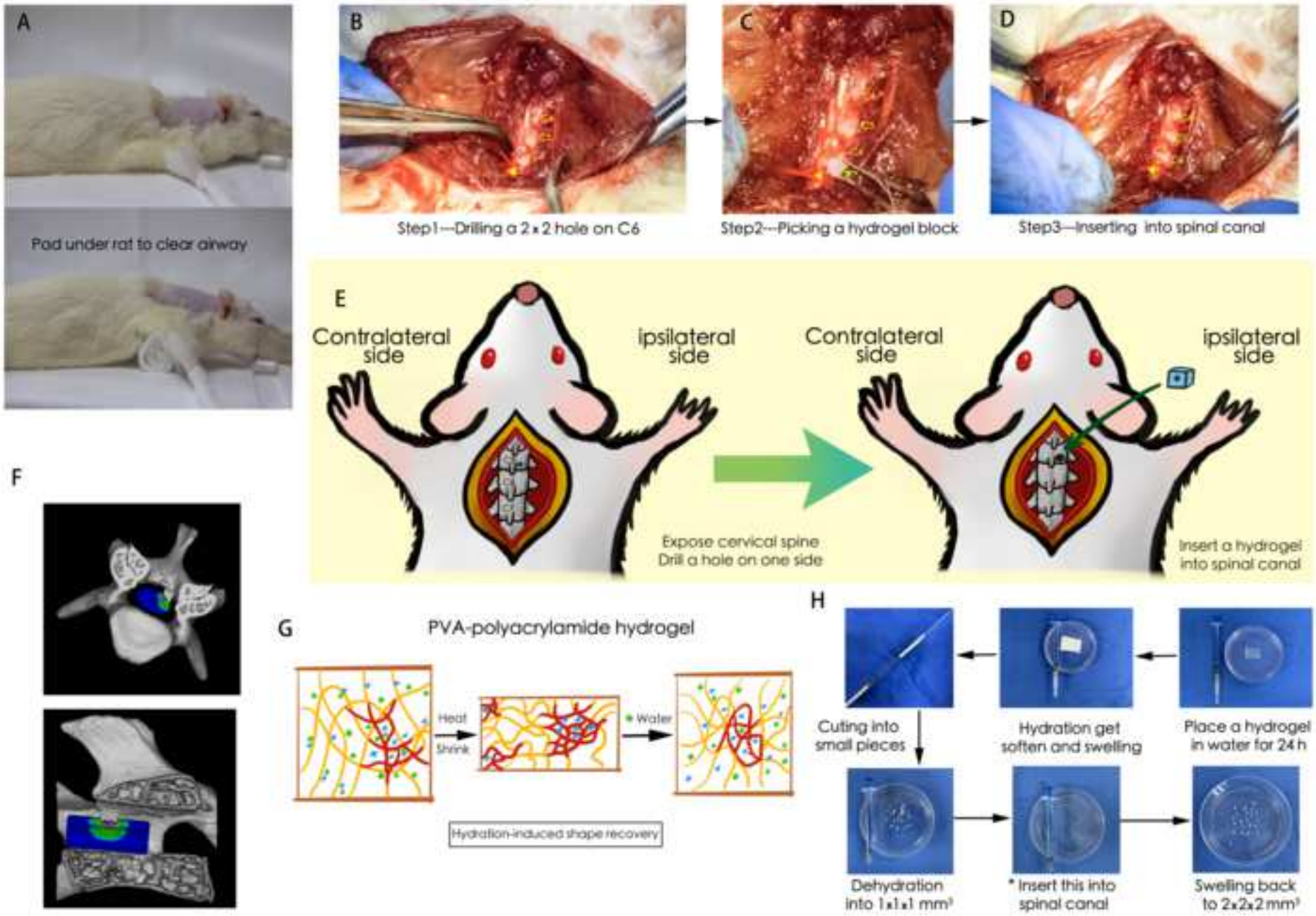

Figure

Click here to access/download;Figure;Jove-Fig2.tif

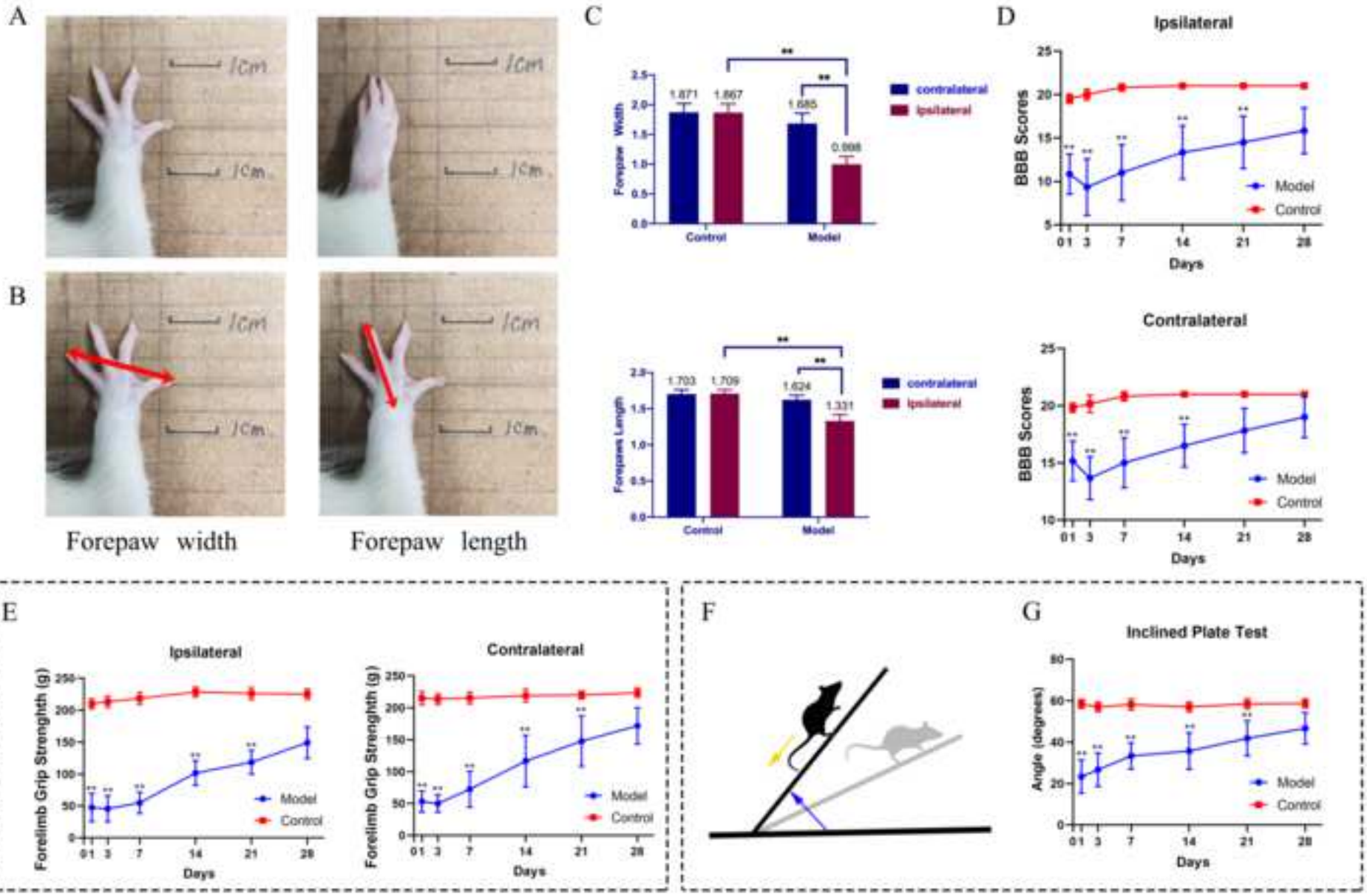

Figure

Click here to access/download;Figure;Jove-Fig3.tif

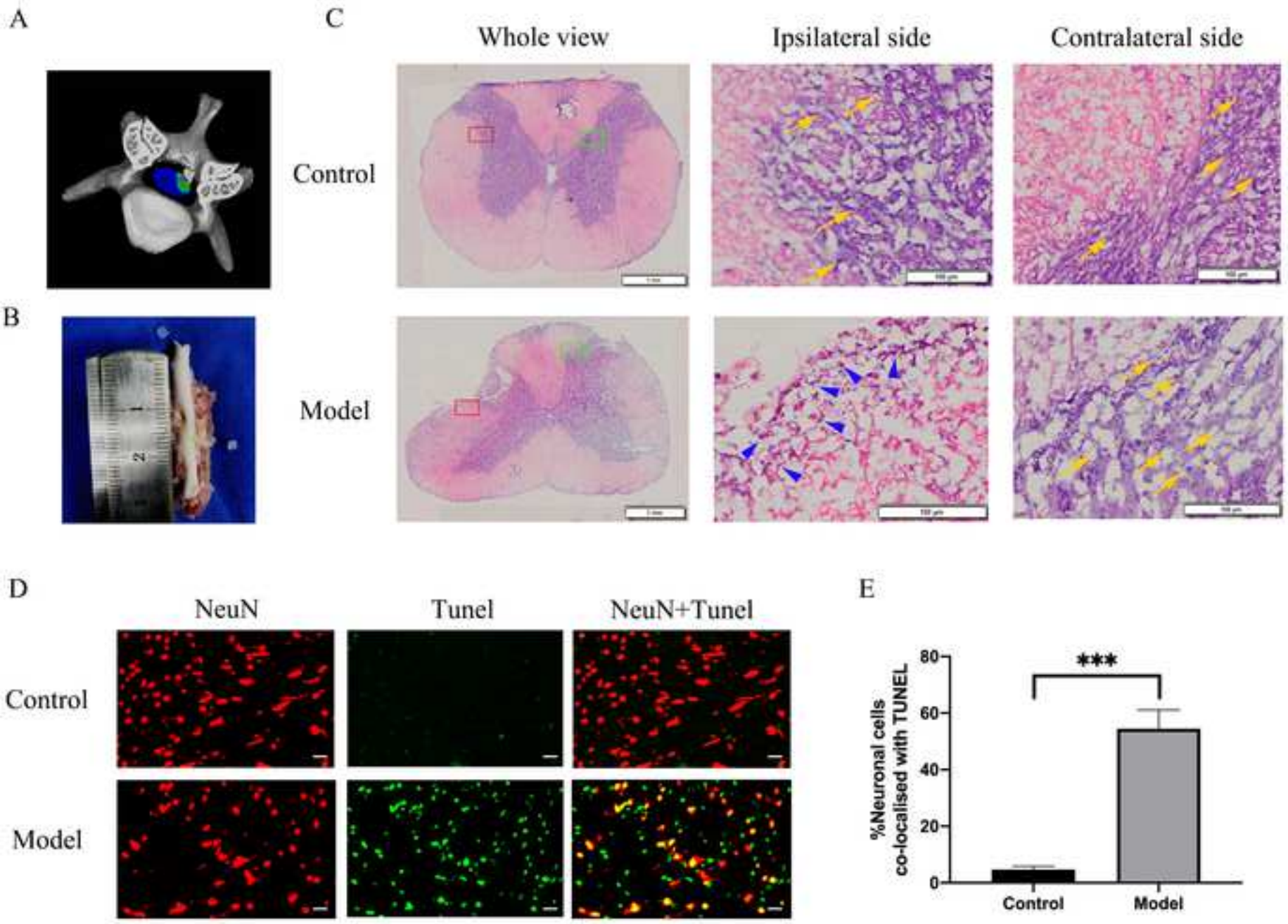

Score	Operational definitions of categories and attributes
0	No observable movement of the hindlimbs
1	Slight (limited) movement of one or two joints, usually hip and/or knee
2	Extensive movement of one joint or extensive movement of one joint and slight movement of the other
3	Extensive movement of two joints
4	Slight movement of all three joints of the hindlimbs
5	Slight movement of two joints and extensive movement of the third joint
6	Extensive movement of two joints and slight movement of the third joint
7	Extensive movement of the three joints in the hindlimbs
8	Sweeping without weight-bearing or plantar support of the paw without weight-bearing
9	Plantar support of the paw with weight-bearing only in the support stage (i.e., when static) or occasional, frequent, or inconsistent dorsal stepping with weight-bearing and no plantar stepping
10	Plantar stepping with occasional weight-bearing and no forelimb-hindlimb coordination
11	Plantar stepping with frequent to consistent weight-bearing and occasional forelimb-hindlimb coordination
12	Plantar stepping with frequent to consistent weight-bearing and occasional forelimb-hindlimb coordination
13	Plantar stepping with frequent to consistent weight-bearing and frequent forelimb-hindlimb coordination
14	Plantar stepping with consistent weight support, consistent forelimb-hindlimb coordination, and predominantly rotated paw position (internally or externally) during locomotion, both at the instant of initial contact with the surface as well as before moving the toes at the end of the support stage or frequent plantar stepping, consistent forelimb-hindlimb coordination, and occasional dorsal stepping

Click here to access/download

Table of Materials

Table of Materials.xlsx

Editorial comments:

Please address the comments inserted in the attached manuscript.

Thanks for all the comments. We have carefully checked and revised in the R2 manuscript.

Reply to reviewer

Reviewer #1:
The authors did a good job addressing the reviewers' concerns. The manuscript reads much clearer now and the redefinition of the injury model was appropriate. Use of buprenorphine and penicillin was a good addition.

Reply: Thank you for your comment. We are glad to introduce this practical model for neural apoptosis studies.

Major concerns:
- Presence and consistency of pathology in the sample population is still unclear (e.g.: line 177-178: "… a notable ipsilateral forepaws' contracture was observed in most of the rats in the model group"
Reply: Thanks for your comment. Except the measurement, we also record the proportion in the two groups, which showed that a notable ipsilateral forepaws' contracture was observed in most of the rats (9/10) in the model group.

Minor concerns:
- Statistical analyses should be described in greater detail for reproducibility (i.e.: tests used, parameters, etc… rather than just reporting the p-value).
Reply: Thanks for your comments. Details in statistical analyses including tests used and parameters has been added in the revised manuscript. Data passed normality testing were analyzed by one-way or two-way analysis with Tukey's test. Data that were not normally distributed but contained equal variances were analyzed with a nonparametric Mann-Whitney U test with post hoc analysis. Data are presented as mean ± standard deviation (SD). Differences were considered statistically significant at $P < 0.05$.

- Clinical relevance of the model, while more appropriately renamed from CSM to cord compression, is unclear. What pathology is this modeling exactly? (e.g.: what does the timeline of injury progression parallel and what conditions should this model be used to investigate?)
Reply: Thank you for your comment. The previous title is too simple to present its use for research. We have changed title as 'A Neural Apoptosis Model induced by Spinal Cord Compression in Rat'

- Some literary and grammar issues still present (e.g.: line 114: "roasting lamp")
Reply: Thank you for your suggestion. All the errors has been checked and revised.

Reply to reviewer

Reviewer #2:

Manuscript Summary:
The authors described a protocol for chronic spinal cord compressive injury model

Major Concerns:
nil

Minor Concerns:
In the introduction part, the authors shall highlight the clinical significance of this experimental endeavour. Below are two relevant clinical research that might help the authors to formulate the clinical needs for this experimental model.

Wen CY, Liu HS, Cui JL, Mak KC, Cheung WY, Hu Y, Luk DK. Is Diffusion Anisotropy A Biomarker for Disease Severity and Surgical Prognosis of Cervical Spondylotic Myelopathy? Radiology 2014 Jan; 270(1):197-204.
Wen CY, Cui JL, Mak KC, Luk DK, Hu Y. Diffusion Tensor Imaging of Somatosensory Tract in Cervical Spondylotic Myelopathy and Its Link with Electrophysiological Evaluation. Spine J 2014 Aug 1;14(8):1493-500.

Based on this experimental model, the in-depth research could be conducted to provide the insight into the underlying mechanism. Below is one of examples for the authors to discuss although no additional immunostaining could be provided at this moment.

Long HQ, Li GS, Hu Y, Wen CY, Xie WH. HIF-1α/VEGF signaling pathway may play a dual role in secondary pathogenesis of cervical myelopathy. Med Hypotheses. 2012 Jul; 79(1): 82-4.

Reply: Thank you for your suggestions. These articles are important to support our introduction. We have added them as references in the revised manuscript.

Reply to reviewer

Reviewer #4:

Manuscript Summary:

The manuscript Sun et al. introduced a new animal model to study the mechanism of neural apoptosis, which plays an important role in the CSM biology field. I'm very glad to review the paper in greater depth because the subject is interesting. And the submission is worth of publication.In addition, this manuscript has been well written in English. I recommend acceptance of this manuscript.

Reply: Thank you for your comment. We are glad to introduce this practical model for neural apoptosis studies.

Major Concerns:

None

Minor Concerns:

None